
STRUCTURE, PHASE TRANSFORMATIONS,
AND DIFFUSION

**Crystallographic Analysis
and Mechanism of the Martensitic Transformation
in the Heusler Alloy $\text{Ni}_{47}\text{Mn}_{42}\text{In}_{11}$**

B. M. Gundyrev^{a,*} and Yu. V. Kaletina^{a,}**

^a*Mikheev Institute of Metals Physics, Ural Branch, Russian Academy of Sciences, Ekaterinburg, 620108 Russia*

^{*}*e-mail: gundyrev@imp.uran.ru*

^{**}*e-mail: kaletina@imp.uran.ru*

Received April 30, 2019; revised May 15, 2019; accepted May 23, 2019

Abstract—The lattice parameters of the matrix of the modulated martensite crystal of the $\text{Ni}_{47}\text{Mn}_{42}\text{In}_{11}$ alloy have been determined. Based on the phenomenological crystallographic theory of martensitic transformations, orientational relationships between the crystal lattices of the martensite matrix and the initial phase have been calculated, and the magnitude and the direction of the macroscopic shear, the habit plane, and the angle and the axis of rotation of the martensite plate have been determined. The mechanism of deformation upon the martensitic transformation has been established.

Keywords: martensitic transformation, martensite matrix, phenomenological theory of martensitic transformations, lattice deformation, shape deformation, average structure of the modulated crystal

DOI: 10.1134/S0031918X19110048

INTRODUCTION

Studies of ferromagnetic alloys have attracted the attention of researchers due to the specific features of their phase transformations, structure formation, and new approaches in studies to such materials. The Ni–Mn–In-based alloys can be separated into a specific group of the so-called Heusler alloys due to the sequence of structural phase transformations occurring in them [1–6] and their potential use in various technological devices. Great attention has been paid in recent years to researching Ni–Mn–In Heusler alloys of nonstoichiometric compositions, in which magnetic-field-controlled shape-memory effects [4, 7] are realized. The investigation of structural and crystallographic peculiarities of martensitic transformations is of interest for determining the influence of structural and magnetic ordering on the functional characteristics of Ni–Mn–In Heusler alloys.

The phenomenological theory of martensitic transformations (PTMTs) describes the formation of a martensite crystal in terms of the product of three matrices: matrix of a Bain deformation (B); deformation (by twinning or slip) with an invariant lattice (P); and rotation (R) [8, 9]. The Bain deformation, which is a pure deformation, transforms the crystal lattice of austenite into the lattice of martensite and is therefore called the lattice deformation. The deformation with an invariant lattice is necessary to obtain the habit

plane of the martensite crystal. The matrix of rotation of the martensite plate describes the rotation that mainly occurs when the austenite lattice is transformed into the martensite lattice. If we consider the real mechanism of deformation of the lattice of the initial phase to the lattice parameters of the martensite, which occurs mainly via shear, then the R matrix will describe only a small rotation that occurs when the martensite is deformed upon an invariant lattice. This was shown in [10–13].

To calculate crystallographic characteristics using the PTMTs it is necessary to know the parameters of the unit cells of the austenite and of the matrix of the martensite. Figure 1a shows a schematic representation of a martensite plate of an iron–nickel alloy with a twinned martensite. Figure 1b shows the unit cell of the modulated structure of $6M$ martensite of the $\text{Ni}_{47}\text{Mn}_{42}\text{In}_{11}$ alloy [14] (as we see, the six-layer structure consists of four layers of the matrix and of two layers in the twinned position). If we make a schematic image of the martensite plate of this alloy, we obtain the same image as in Fig. 1a. However, the thickness of the portions of the matrix and of the twins in the twinned martensite of the iron–nickel alloy is approximately 100–1000 times greater than in the modulated martensite. In the twinned martensite, the twins and the regions of the martensite matrix located between the twins scatter X-rays independently of each other,

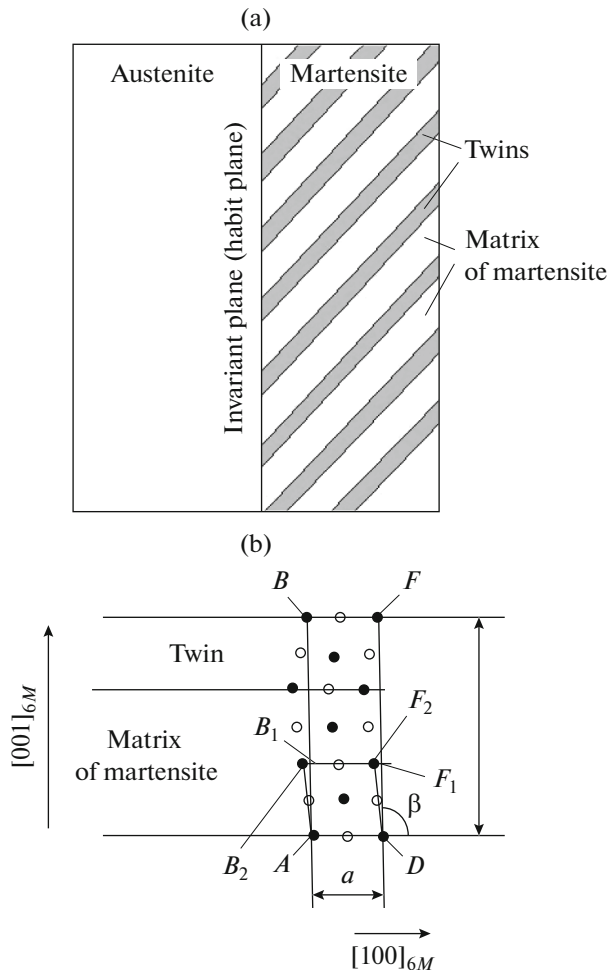


Fig. 1. (a) A schematic representation of a martensite plate of an Fe–Ni alloy and (b) the unit cell of the $6M$ martensite lattice of the alloy $\text{Ni}_{47}\text{Mn}_{42}\text{In}_{11}$. AB_2F_2D is the unit cell of the martensite matrix; AB_1F_1D is the unit cell of the averaged martensite structure (basic cell); B_1 , the point of intersection of lines AB and B_2F_2 ; F_1 , the point of intersection of lines DF and of the straight line B_2F_2 ; $ABFD$, the unit cell of the modulated structure of the $6M$ martensite.

and the experimentally determined unit cell of the martensite lattice is the unit cell of the martensite matrix. In the case of the modulated martensite, the volume of a coherent-scattering region (CSR) involves a large number of alternating regions of the matrix and twins. The diffraction pattern obtained from such a CSR corresponds to a crystal lattice with a new unit cell (the unit cell of the modulated structure of martensite), including at least one region of the matrix and one twin. If we exclude the satellites present in the XRD patterns, we obtain a diffraction pattern corresponding to an “averaged” structure. The unit cell of such an averaged structure (basic unit cell) differs significantly from the unit cell of the matrix of the martensite, as can be seen in Fig. 1b. Based on the known parameters of the unit cell of the modulated structure

of martensite, or on the parameters of the basic unit cell, it is possible to find the crystallographic characteristics of martensite using the PTMTs, as was done in [15] for the modulated 63.0 Ni–37.0 Al (at %) alloy, but the mechanism of deformation of the lattice upon the martensitic transformation cannot be determined. To determine this mechanism using the PTMTs, it is necessary to know the parameters of the unit cell of the martensite matrix, which cannot be obtained directly from XRD measurements, but can be calculated based on the known parameters of the unit cell of the modulated structure.

The aim of this work is to determine the unit cell of the martensite matrix and the mechanism of lattice deformation upon the martensitic transformation in the $\text{Ni}_{47}\text{Mn}_{42}\text{In}_{11}$ alloy, as well as to determine the crystallographic characteristics of the martensite using the PTMTs.

DETERMINATION OF PARAMETERS OF THE UNIT CELL OF MARTENSITE MATRIX

We determined in [14] the parameters of the unit cell of the modulated monoclinic structure of the $\text{Ni}_{47}\text{Mn}_{42}\text{In}_{11}$ alloy as $a = 0.4406$ nm, $b = 0.5601$ nm, $c = 1.3024$ nm, and $\beta = 93.51^\circ$. As can be seen from Fig. 1b, the cell contains six layers, with four layers of atoms belonging to the matrix and two layers belonging to the twin. Figure 2 provides an auxiliary drawing for determining the parameters of the unit cell of the martensite matrix. The rectangular OLK and OAB triangles can be used to do this. From the OLK triangle, we find $OK = c \cos \delta$, $LK = c \sin \delta$. Taking into account that $AB = LK$ and $OB = OK/3$, we find c_1 and δ_1 :

$$c_1 = c\sqrt{\sin^2 \delta + (\cos^2 \delta)/9}$$
 and $\delta_1 = \arctan(3 \tan \delta)$. As a result of calculations, we obtain: $a_1 = a = 0.44053$ nm, $b_1 = b = 0.56013$ nm, $c_1 = 0.44064$ nm, $\beta_1 = 90^\circ + \delta_1 = 100.43^\circ$. Thus, we find the parameters of the monoclinic cell of the martensite matrix: $a_1 = c_1 = 0.4406 \pm 0.0001$ nm, $b_1 = 0.5601 \pm 0.0001$ nm, $\beta_1 = 100.43^\circ \pm 0.01^\circ$. As can be seen, $a_1 = c_1$. This indicates that the lattice of the martensite matrix is orthorhombic. Therefore, we pass to the orthorhombic axes, as shown in Fig. 2, and find the unit cell of the martensite matrix: $a_2 = 0.5601 \pm 0.0001$ nm, $b_2 = 0.5639 \pm 0.0001$ nm, $c_2 = 0.6771 \pm 0.0001$ nm. It could be expected that the unit cell of the martensite matrix should be more symmetrical than the unit cell of the modulated martensite structure, since the latter includes a structural defect in the form of a twin. Indeed, we obtained a more symmetrical (orthorhombic) cell close to a tetragonal cell.

CALCULATION
OF CRYSTALLOGRAPHIC PARAMETERS
OF MARTENSITE USING THE PTMTs

For calculations, we take the lattice parameter of the initial cubic phase $a_0 = 0.5998$ nm, and the parameters of the lattice of the final orthorhombic phase $a = 0.5601$ nm, $b = 0.5639$ nm, and $c = 0.6771$ nm. The pure deformation of the cubic lattice to obtain this orthorhombic lattice is chosen from the equivalent variants as follows:

$$B_0 = \begin{pmatrix} 0.5601 & 0 & 0 \\ 0.5998 & & \\ 0 & 0.5639 & 0 \\ & 0.5998 & \\ 0 & 0 & 0.6771 \\ & & 0.5998 \end{pmatrix} \quad (1)$$

This pure deformation of the lattice can be obtained by shear along the plane (112) in the direction $[\bar{1}\bar{1}1]$ by 0.18503 and then by stretching along the direction $[\bar{1}\bar{1}1]$ by 0.5%, compression along $[1\bar{1}0]$ by 6.4%, and stretching along $[112]$ by 5.3%. The matrix that describes the shear Γ in this case is as follows:

$$\Gamma = T^{-1} \cdot \begin{pmatrix} 1 & 0 & 0.18503 \\ 0 & 1 & 0 \\ 0 & 0 & 1 \end{pmatrix} \cdot T, \quad (2)$$

where

$$T = \begin{pmatrix} \frac{-1}{\sqrt{3}} & \frac{-1}{\sqrt{3}} & \frac{1}{\sqrt{3}} \\ \frac{1}{\sqrt{2}} & \frac{-1}{\sqrt{2}} & 0 \\ \frac{1}{\sqrt{6}} & \frac{1}{\sqrt{6}} & \frac{2}{\sqrt{6}} \end{pmatrix}$$

is the matrix of rotation of the coordinate axes, and T^{-1} is the inverse matrix.

The matrix of the additional strain B_1 has the following form:

$$B_1 = T^{-1} \cdot \begin{pmatrix} 1.00505 & 0 & 0 \\ 0 & 0.93700 & 0 \\ 0 & 0 & 1.05247 \end{pmatrix} \cdot T.$$

Thus, the deformation of the lattice can be calculated as follows:

$$B = B_2 B_1 \Gamma. \quad (3)$$

Here, $B_2 = \begin{pmatrix} 0.99668 & 0 & -0.00021 \\ 0 & 1.00333 & 0.00021 \\ -0.00021 & 0.00021 & 1 \end{pmatrix}$ is a correction related to the orthorhombic distortions of the lattice.

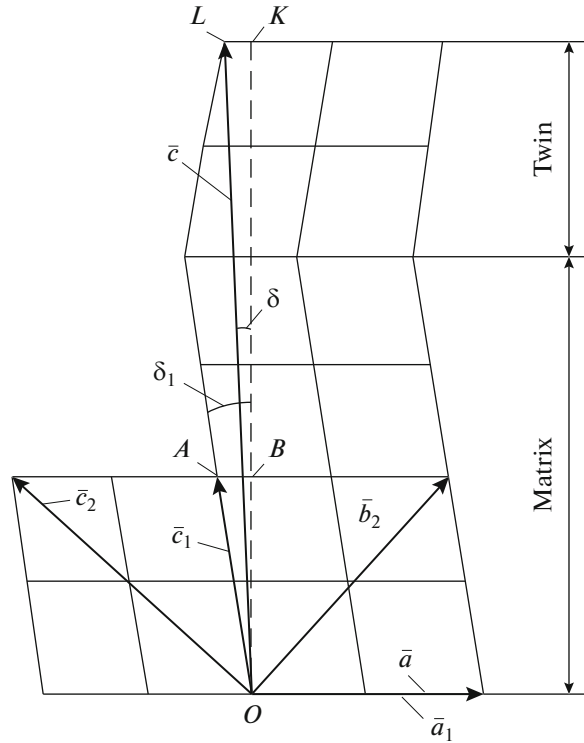


Fig. 2. Scheme for the determination of the lattice parameters of the martensite matrix. The scheme is given in a plane perpendicular to the unit vector \bar{b} ; $\bar{a}, \bar{b}, \bar{c}$, and $\beta = 90^\circ + \delta$ are the parameters of the unit cell of the modulated structure of martensite; $\bar{a}_1, \bar{b}_1, \bar{c}_1$, $\beta_1 = 90^\circ + \delta_1$, the parameters of the monoclinic unit cell of the martensite matrix; $\bar{a}_2, \bar{b}_2, \bar{c}_2$, the parameters of the orthorhombic unit cell of the martensite matrix; $\bar{b} = \bar{b}_1 = -\bar{a}_2$, $\bar{a} = \bar{a}_1$.

To obtain the habit plane, we introduce into the calculations the invariant-lattice deformation P by twinning of the martensite, as is done in the FTPMs. A system should be chosen from the twinning systems that results in a minimum deformation of the shape (P_1) of the martensite plate. Figure 3 shows that for the chosen deformation of the lattice upon the martensite transformation by shear along the plane (112) $L2_1$ in the direction $[\bar{1}\bar{1}1]L2_1$ there are two equivalent twinning systems: (101)[10 $\bar{1}$] and (011)[01 $\bar{1}$]. Thus, for each of the 12 variants of the lattice deformation, we have two variants of invariant-lattice deformation of martensite; as a result, we have 24 martensite orientations, as shown in Table 1.

The crystallographic analysis is carried out for the case of the orientation no. 5, since the calculations for this orientation are simpler. The matrix P of the martensite deformation is as follows:

$$P = S^{-1} \cdot \begin{pmatrix} 1 & 0 & g \\ 0 & 1 & 0 \\ 0 & 0 & 1 \end{pmatrix} \cdot S. \quad (4)$$

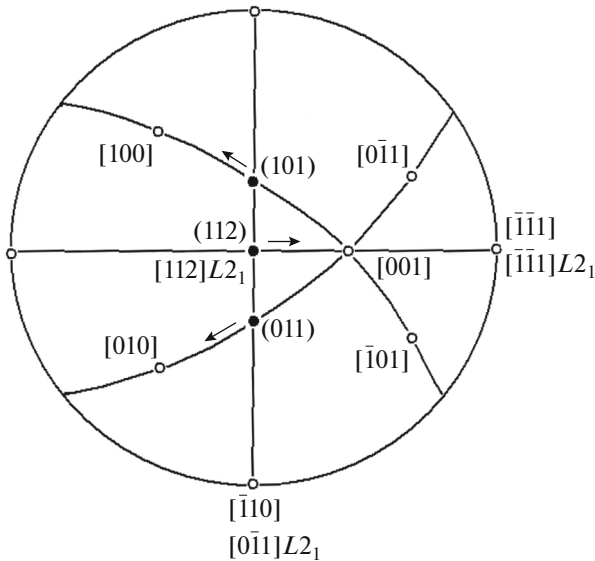


Fig. 3. Stereographic projection of the twinning systems in the orthorhombic lattice of the martensite matrix for the shear variant, in which the orientation relationships $[111]L_{2_1} \parallel [111]R$ and $(\bar{1}\bar{1}2) L_{2_1} \parallel (\bar{1}\bar{1}2)R$ are fulfilled.

Choose the twinning in the system $(011)[01\bar{1}]$; in this case,

$$S = \begin{pmatrix} 0.04761 & 0.68754 & -0.72458 \\ -0.99797 & 0.00203 & -0.06365 \\ -0.04229 & 0.72614 & 0.68624 \end{pmatrix}$$

is the matrix of rotation of the coordinate axes from the initial coordinates of the austenite lattice to the orthogonal coordinates chosen in the orthorhombic lattice of martensite in such a way that the X axis be coincident with the shear direction $[01\bar{1}]R$, the Z axis be coincident with the normal to the plane $(011)R$, and the Y axis be perpendicular to them.

As was mentioned above, the XRD structural studies allow one to directly find the basic cell in the modulated martensite crystal. Figure 2 shows that the basic cell does not coincide with the unit cell of the martensite matrix. This gives two orientation relationships relative to the initial phase: one for the lattice of the martensite matrix, and the second one for the lattice of the averaged structure of the modulated martensite crystal. The first matrix (θ_1) to determine the indices of the direction $[uvw]$ in the L_{2_1} lattice, which is parallel to the direction $[UVW]$ in the orthorhombic lattice of the martensite matrix, is calculated as follows: $\theta_1 = RB$. The second matrix (θ_2) for the determination of the indices of the direction $[uvw]$ in the L_{2_1} lattice

that is parallel to the direction $[UVW]$ in the averaged martensite lattice is calculated as $\theta_2 = RDB$, where

$$D = S^{-1} \cdot \begin{pmatrix} 1 & 0 & g_1 \\ 0 & 1 & 0 \\ 0 & 0 & 1 \end{pmatrix} \cdot S$$

The value of g_1 is determined from Fig. 2:

$$g_1 = \tan(\delta_1) - \tan(\delta) = 0.12268. \quad (5)$$

The matrix D describes the invariant-lattice deformation of martensite within a CSR. Further calculations of the crystallographic characteristics of the martensite were made in full agreement with the PTMTs [1, 2].

The results for the three variants of calculations of the crystallographic characteristics of martensite transformation are presented in Table 2.

ANALYSIS OF THE RESULTS

The PTMTs makes it possible to find various crystallographic parameters of the transformation, e.g., the habit plane, orientation relationships, shape deformation, etc. To do this, it is sufficient to know the parameters of the unit cell of the initial phase, the lattice parameters of the final phase, and the mechanism of invariant-lattice deformation of the martensite. In the first and second variants of the calculation, the unit cell of the martensite matrix is selected as the unit cell of the final phase. In the third variant, the unit cell of the modulated structure of martensite is chosen as such a cell, which, in addition to the matrix, includes a twin. Such a choice of the unit cell of the final phase was used in [15] for the crystallographic analysis of the martensitic transformation $B2 \rightarrow 7R$ in the Ni–37.0 at % Al.

In the first variant, the uniform deformation of the lattice is described by Eq. (3). In the second variant, as the mechanism of a homogeneous deformation of the lattice, the Bain deformation is used, containing only a pure lattice deformation without rotation elements. This makes it possible to obtain crystallographic characteristics of the martensitic transformation, but does not allow us to find the real mechanism of martensitic transformation, unlike the first variant. When choosing a realistic mechanism of martensitic transformation, the angle φ should be small. In the first variant, the angle φ is only 0.36° . In the second and third variants, unrealistic large values of the angle φ are obtained. Therefore, only the first variant corresponds to a real mechanism of the lattice deformation. This mechanism, as can be seen from calculations, consists in a shear in the plane (112) in the direction $[\bar{1}\bar{1}1]$ by 0.185 and in an additional pure deformation, which consists in a stretching by 5.3% in the direction of the normal to the shear plane, stretching by 0.5% in the shear direction, and compression by 6.4% in the third direction $[01\bar{1}]$ perpendicular to the first two. As is

Table 1. Orientations and corresponding shear systems in the initial phase and the twinning systems in martensite

Order number of orientation	Initial phase		Martensite	
	(hkl) $L2_1$	$[uvw]$ $L2_1$	(HKL) R	$[UVW]$ R
1	211	$\bar{1}\bar{1}\bar{1}$	101	$\bar{1}01$
2	$\bar{2}\bar{1}\bar{1}$	$\bar{1}\bar{1}\bar{1}$	$\bar{1}01$	101
3	$12\bar{1}$	$\bar{1}\bar{1}1$	$01\bar{1}$	$0\bar{1}\bar{1}$
4	$\bar{1}\bar{2}\bar{1}$	$\bar{1}\bar{1}1$	$0\bar{1}\bar{1}$	$01\bar{1}$
5	112	$\bar{1}\bar{1}1$	011	$01\bar{1}$
6	$\bar{1}\bar{2}\bar{1}$	111	$\bar{1}10$	$\bar{1}\bar{1}0$
7	$\bar{1}\bar{1}\bar{2}$	$\bar{1}\bar{1}\bar{1}$	$01\bar{1}$	011
8	$\bar{1}\bar{2}\bar{1}$	$\bar{1}\bar{1}\bar{1}$	$\bar{1}\bar{1}0$	$\bar{1}10$
9	121	$\bar{1}\bar{1}\bar{1}$	110	$\bar{1}\bar{1}0$
10	$\bar{1}\bar{1}\bar{2}$	111	$0\bar{1}1$	$0\bar{1}\bar{1}$
11	$1\bar{1}\bar{2}$	$\bar{1}\bar{1}\bar{1}$	$0\bar{1}\bar{1}$	$0\bar{1}1$
12	$1\bar{2}\bar{1}$	$\bar{1}\bar{1}\bar{1}$	$\bar{1}\bar{1}0$	110
13	$2\bar{1}\bar{1}$	$\bar{1}\bar{1}\bar{1}$	110	$\bar{1}\bar{1}0$
14	$\bar{1}\bar{1}\bar{2}$	$\bar{1}\bar{1}\bar{1}$	$\bar{1}01$	$\bar{1}0\bar{1}$
15	$\bar{2}\bar{1}\bar{1}$	$\bar{1}\bar{1}\bar{1}$	$\bar{1}\bar{1}0$	110
16	$\bar{1}\bar{1}\bar{2}$	111	$\bar{1}0\bar{1}$	$\bar{1}01$
17	$2\bar{1}\bar{1}$	111	$\bar{1}\bar{1}0$	$\bar{1}\bar{1}0$
18	$\bar{1}\bar{1}\bar{2}$	$\bar{1}\bar{1}\bar{1}$	101	$10\bar{1}$
19	$\bar{2}\bar{1}\bar{1}$	$\bar{1}\bar{1}\bar{1}$	$\bar{1}\bar{1}0$	$\bar{1}\bar{1}0$
20	$1\bar{1}\bar{2}$	$\bar{1}\bar{1}\bar{1}$	$10\bar{1}$	101
21	$\bar{2}\bar{1}\bar{1}$	$\bar{1}\bar{1}\bar{1}$	$\bar{1}0\bar{1}$	$10\bar{1}$
22	$2\bar{1}\bar{1}$	111	$10\bar{1}$	$\bar{1}0\bar{1}$
23	$\bar{1}\bar{2}\bar{1}$	$\bar{1}\bar{1}\bar{1}$	011	$0\bar{1}\bar{1}$
24	$1\bar{2}\bar{1}$	$\bar{1}\bar{1}\bar{1}$	$0\bar{1}\bar{1}$	011

Table 2. Calculated crystallographic parameters of the martensitic transformation

Parameters	Shear mechanism ¹	Bain mechanism ¹	Bain mechanism ²
<i>B</i>	$\begin{pmatrix} 0.93197 & -0.00191 & -0.07186 \\ -0.0019 & 0.93821 & -0.07185 \\ 0.05944 & 0.05984 & 1.12431 \end{pmatrix}$	$\begin{pmatrix} 0.93386 & 0 & 0 \\ 0 & 0.94011 & 0 \\ 0 & 0 & 1.12889 \end{pmatrix}$	$\begin{pmatrix} 0.93386 & 0 & 0 \\ 0 & 0.99889 & -0.03991 \\ 0 & 0.02276 & 1.06156 \end{pmatrix}$
<i>P</i>	$\begin{pmatrix} 0.99975 & 0.00437 & 0.00413 \\ -0.00366 & 1.0631 & 0.05965 \\ 0.00387 & -0.0665 & 0.93714 \end{pmatrix}$	$\begin{pmatrix} 1 & 0 & 0 \\ 0 & 1.06217 & 0.05177 \\ 0 & -0.07465 & 0.93783 \end{pmatrix}$	$\begin{pmatrix} 1 & 0 & 0 \\ 0 & 1.00187 & 0.00187 \\ 0 & -0.00187 & 0.99813 \end{pmatrix}$
<i>R</i>	$\begin{pmatrix} 0.99998 & 0.00616 & 0.00046 \\ -0.00616 & 0.99998 & 0.00113 \\ -0.00044 & -0.00113 & 1 \end{pmatrix}$	$\begin{pmatrix} 0.99797 & 0.00415 & -0.06358 \\ -0.00811 & 0.99803 & -0.06214 \\ 0.06319 & 0.06253 & 0.99604 \end{pmatrix}$	$\begin{pmatrix} 0.99797 & 0.0099 & -0.06294 \\ -0.0081 & 0.99955 & 0.0288 \\ 0.0632 & -0.02824 & 0.9976 \end{pmatrix}$
<i>g</i>	0.12642		0.00374
<i>P</i> ₁	$\begin{pmatrix} 0.93196 & 0.00860 & -0.06707 \\ -0.00757 & 1.00096 & -0.00746 \\ 0.05902 & -0.00746 & 1.05818 \end{pmatrix}$		
Habit plane	(0.7093; -0.0897; 0.6992)		
Shear direction	[-0.7527; -0.0837; 0.6529]		
Shear magnitude	0.12743		
θ_1	$\begin{pmatrix} 0.93196 & 0.00390 & -0.07178 \\ -0.00757 & 0.93827 & -0.07015 \\ 0.05902 & 0.05878 & 1.12443 \end{pmatrix}$		
θ_2	$\begin{pmatrix} 0.93196 & 0.00846 & -0.06721 \\ -0.00757 & 0.99910 & -0.00932 \\ 0.05902 & -0.00550 & 1.06014 \end{pmatrix}$		
<i>u</i>	[-0.179; 0.073; -0.981]	[0.699; -0.711; -0.069]	[-0.409; -0.904; -0.129]
φ , degrees	0.36	5.11	4.00

¹ The calculation is made relative to the unit cell of the martensite matrix.

² The calculation is made relative to the basic unit cell of the martensite; *u* is the direction of the axis of rotation of the martensite plate by an angle φ in the coordinate system of the $L2_1$ lattice.

known, the shear systems of the $\{112\}\langle\bar{1}\bar{1}\bar{1}\rangle$ family are typical of bcc crystals. There are 12 such equivalent shear systems.

Taking into account Eq. (5), we find for the first variant $g_2 = g - g_1 = 0.00374$. Since g_1 is the invariant-lattice shear deformation of the martensite matrix within a CSR, the g_2 is a displacement of the CSRs relative to each other. For the third variant, we obtain $g = g_2$, which is equal to only 3% of the magnitude of g for the first variant.

In [14], we experimentally determined the orientation relationships for the basic lattice of the martensite relative to the initial phase: $(110)L2_1 \parallel (12\bar{1})6M$ and $[\bar{1}10]L2_1 \parallel [\bar{1}11]6M$ (with an error of 0.5°). These orientation relationships refer to orientation no. 2 in Table 1. For this orientation, the calculated plane $(12\bar{1})6M$ deviates from the plane $(110)L2_1$ by 0.13° and the calculated direction $[\bar{1}11]6M$ deviates from the direction $[\bar{1}10]L2_1$ by 0.08° . Thus, the calculated ori-

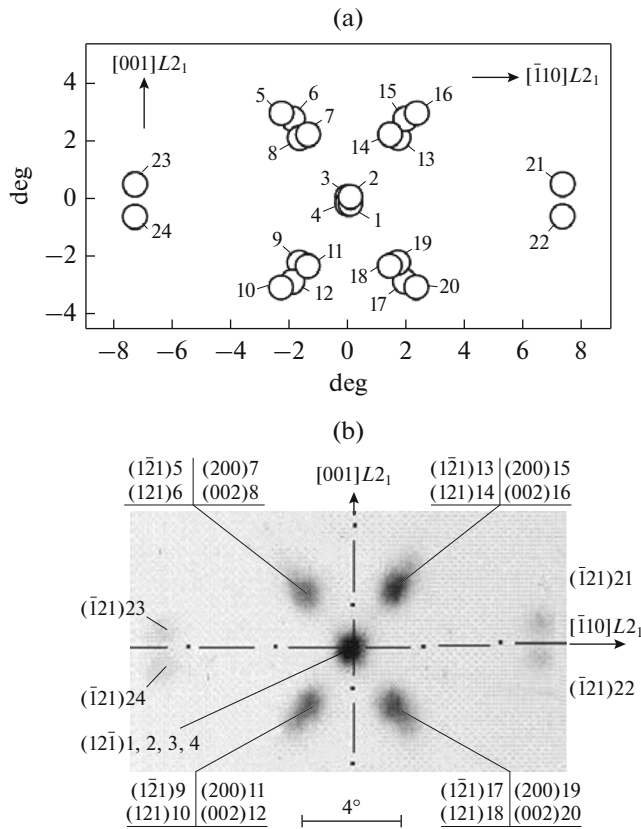


Fig. 4. (a) Fragment of the stereographic projection showing the poles of the crystallographic planes of martensite that originate from the plane $(110)L2_1$ upon the martensitic transformation; and (b) the XRD pattern of texture maxima obtained in the vicinity of the pole $(110)L2_1$. The numbers 1 to 24 correspond to the order numbers of orientations.

entation relationships of the basic lattice completely correspond to those found experimentally. A similar conclusion can also be drawn from the comparison of the calculated and experimental pictures in Fig. 4.

CONCLUSIONS

(1) The parameters of the unit cell of the matrix of the modulated martensite crystal in the Heusler alloy $\text{Ni}_{47}\text{Mn}_{42}\text{In}_{11}$ have been determined to be $a = 0.5601$ nm, $b = 0.5639$ nm, $c = 0.6771$ nm, $\alpha = 90^\circ$, $\beta = 90^\circ$, and $\gamma = 90^\circ$.

(2) Based on the phenomenological crystallographic theory of martensitic transformations, the orientation relationships between the crystal lattices of the martensite matrix and the initial phase $L2_1$, as well as between the lattice of the averaged martensite structure and that of the initial phase, have been calculated. The magnitude and the direction of the macroscopic shear, the habit plane, the angle and the axis of rotation of the martensite plate have been determined.

(3) The mechanism of deformation upon martensitic transformation has been established to be as follows: a shear in the plane (112) in the direction $[\bar{1}\bar{1}1]$ by 0.185% in the initial $L2_1$ phase and an additional stretching by 5.3% in the direction of the normal to the shear plane, stretching by 0.5% in the shear direction, and a compression by 6.4% in the transverse direction.

Thus, the shear mechanism we used, just as the Bain deformation, make it possible to obtain the lattice of the martensite. The advantage of the shear mechanism is that it not only deforms the lattice, but also rotates it by an angle that corresponds to the angle of the lattice rotation upon the martensitic transformation.

ACKNOWLEDGMENTS

The authors are grateful to Dr. V.I. Zeldovich for a useful discussion of the results and for providing valuable advice.

FUNDING

The work was carried out within the framework of the State task according to the themes “Struktura” No. AAAA-A18-118020190116-6 and “Davlenie” No. AAAA-A18-118020 190104-3.

REFERENCES

1. Y. Sutou, Y. Imano, N. Koeda, T. Omori, R. Kainuma, K. Ishida, and K. Oikawa, “Magnetic and martensitic transformations of NiMnX ($X = \text{In, Sn, Sb}$) ferromagnetic shape memory alloys,” *Appl. Phys. Lett.* **85**, No. 19, 4358–4360 (2004).
2. T. Krenke, M. Acet, E. Wassermann, L. Manosa, and A. Planes, “Ferromagnetism in the austenitic and martensitic states of Ni-Mn-In alloys,” *Phys. Rev. B* **73**, 174413 (2006).
3. T. Krenke, E. Duman, M. Acet, E. F. Wassermann, L. Manosa, and A. Planes, “Magnetic superelasticity and inverse magnetocaloric effect in Ni-Mn-In ,” *Phys. Rev. B* **74**, 104414 (2007).
4. V. D. Buchelnikov and V. V. Sokolovskiy, “Magnetocaloric effect in Ni-Mn-X ($X = \text{Ga, In, Sn, Sb}$) Heusler alloys,” *Phys. Met. Metallogr.* **112**, No. 7, 633–665 (2011).
5. V. M. Schastlivtsev, Yu. V. Kaletina, and E. A. Fokina, *Martensitic Transformation in Magnetic Field* (UrO RAN, Yekaterinburg, 2007) [in Russian].
6. V. M. Schastlivtsev, Yu. V. Kaletina, E. A. Fokina, and V. A. Kazantsev, “Martensitic and magnetic transformations in Ni-Mn-In alloys,” *Phys. Met. Metallogr.* **112**, No. 1, 61–71 (2011).
7. Yu. V. Kaletina and E. G. Gerasimov, “Martensitic transformations and magnetic properties of nonstoichiometric alloys of the Ni-Mn-In system,” *Phys. Solid State* **56**, No. 8, 1634–1638 (2014).

8. M. S. Wechsler, D. S. Lieberman, and T. A. Read, "On the theory of the formation of martensite," *Trans. AIME* **197**, 1503 (1953).
9. C. M. Wayman, *Introduction to the Crystallography of Martensitic Transformations* (New York, 1964).
10. V. M. Gundyrev and V. I. Zel'dovich, "Crystallographic analysis of the $B2 \rightarrow B19'$ martensite transformation in titanium nickelide," *Bull. Russ. Acad. Sci.: Phys.* **76**, No. 1, 18–22 (2012).
11. V. M. Gundyrev and V. I. Zeldovich, "Crystallographic analysis of martensitic transformation in an iron-nickel alloy with twinned martensite," *Bull. Russ. Acad. Sci.: Phys.* **77**, No. 11, 1367–1372 (2013).
12. V. M. Gundyrev and V. I. Zel'dovich, "Crystallographic analysis of the FCC \rightarrow BCC martensitic transformation in high-carbon steel," *Phys. Met. Metallogr.* **115**, No. 10, 973–980 (2014).
13. V. M. Gundyrev, V. I. Zel'dovich, and V. M. Schastlivtsev, "Crystallographic analysis of the martensitic transformation in medium-carbon steel with packet martensite," *Phys. Met. Metallogr.* **117**, No. 10, 1017–1027 (2016).
14. V. M. Gundyrev and Yu. V. Kaletina, "X-Ray diffraction study of the martensite structure of the $Ni_{47}Mn_{42}In_{11}$ alloy" *Phys. Met. Metallogr.* **119**, No. 10, 962–968 (2018).
15. Y. Murakami, K. Otsuka, S. Hanada, and S. Watanabe, "Crystallography of stress-induced $B2-7R$ martensitic transformation in a Ni–37.0 at % Al alloy," *Mater. Trans., JIM* **33**, 282–288 (1992).

Translated by S. Gorin